

Received 3 December 2019  
Accepted 17 December 2019

Edited by A. J. Lough, University of Toronto,  
Canada

**Keywords:** crystal structure; dihydrobenzodiazole; hydrogen bond; triazole;  $\pi$ -stacking; Hirshfeld surface.

**CCDC reference:** 1972575

**Supporting information:** this article has supporting information at journals.iucr.org/e

# Crystal structure, Hirshfeld surface analysis and DFT studies of 1-benzyl-3-[(1-benzyl-1H-1,2,3-triazol-5-yl)methyl]-2,3-dihydro-1H-1,3-benzodiazol-2-one monohydrate

Asmaa Saber,<sup>a</sup> Nada Kheira Sebbar,<sup>b,a\*</sup> Tuncer Hökelek,<sup>c</sup> Mohamed Labd Taha,<sup>b</sup> Joel T. Mague,<sup>d</sup> Noureddine Hamou Ahabchane<sup>a</sup> and El Mokhtar Essassi<sup>a</sup>

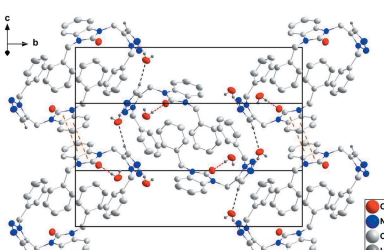
<sup>a</sup>Laboratoire de Chimie Organique Hétérocyclique URAC 21, Pôle de Compétence Pharmacochimie, Av. Ibn Battouta, BP 1014, Faculté des Sciences, Université Mohammed V, Rabat, Morocco, <sup>b</sup>Laboratoire de Chimie Appliquée et Environnement, Equipe de Chimie Bioorganique Appliquée, Faculté des Sciences, Université Ibn Zohr, Agadir, Morocco,

<sup>c</sup>Department of Physics, Hacettepe University, 06800 Beytepe, Ankara, Turkey, and <sup>d</sup>Department of Chemistry, Tulane University, New Orleans, LA 70118, USA. \*Correspondence e-mail: nadouchsebbarkheira@gmail.com

In the title molecule,  $C_{24}H_{21}N_5O \cdot H_2O$ , the dihydrobenzodiazole moiety is not quite planar, while the whole molecule adopts a U-shaped conformation in which there is a close approach of the two benzyl groups. In the crystal, chains of alternating molecules and lattice water extending along [201] are formed by  $O - H_{\text{UncoordW}} \cdots O_{\text{Dhyr}}$  and  $O - H_{\text{UncoordW}} \cdots N_{\text{Trz}}$  ( $\text{UncoordW}$  = uncoordinated water, Dhyr = dihydro and Trz = triazole) hydrogen bonds. The chains are connected into layers parallel to (010) by  $C - H_{\text{Trz}} \cdots O_{\text{UncoordW}}$  hydrogen bonds with the dihydrobenzodiazole units in adjacent layers intercalating to form head-to-tail  $\pi$ -stacking [centroid-to-centroid distance = 3.5694 (11) Å] interactions between them, which generates the overall three-dimensional structure. Hirshfeld surface analysis indicates that the most important contributions for the crystal packing are from  $H \cdots H$  (52.1%),  $H \cdots C/C \cdots H$  (23.8%) and  $O \cdots H/H \cdots O$  (11.2%) interactions. Hydrogen-bonding and van der Waals interactions are the dominant interactions in the crystal packing. Density functional theory (DFT) optimized structures at the B3LYP/ 6–311 G(d,p) level are compared with the experimentally determined molecular structure in the solid state. The HOMO–LUMO behaviour was elucidated to determine the energy gap.

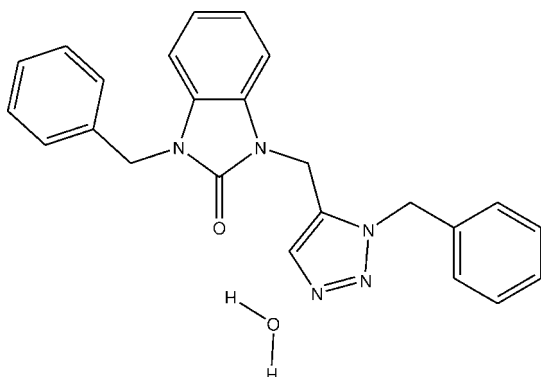
## 1. Chemical context

Nitrogen heterocyclic compounds are known to exhibit excellent biological and pharmaceutical activities (Olesen *et al.*, 1994; Baxter & Clarke, 1992; Saber *et al.*, 2020; Rémond *et al.*, 1997). The benzimidazole core has several active sites and provides great responsiveness, making it an excellent heterocyclic precursor in the syntheses of the new heterocyclic compounds (Saber *et al.*, 2018*a,b*; Ouzidan *et al.*, 2011; Saber *et al.*, 2020). With respect to the biological applications of benzimidazolone derivatives, it has been shown that these compounds are found to possess potent antioxidant (Gaba *et al.*, 2014), antiparasitic (Ayhan-Kilcigil *et al.*, 2007), anthelmintic (Navarrete-Vazquez *et al.*, 2001), antiproliferative (Ravina *et al.*, 1993), anti-HIV (Garuti *et al.*, 2000), anti-convulsant (Rao *et al.*, 2002), anti-inflammatory (Thakurdesai *et al.*, 2007), antihypertensive (Serafin *et al.*, 1989) and anti-trichinellosis (Mavrova *et al.*, 2007) activities. In addition, they are considered to be important moieties for the development of molecules of pharmaceutical interest (Mondieig *et al.*, 2013;



OPEN ACCESS

Lakhrissi *et al.*, 2008). As a continuation of our research devoted to the study of cycloaddition reactions involving benzimidazolone derivatives (Sebbar *et al.*, 2016; Saber *et al.*, 2020), we report herein the synthesis, the molecular and crystal structures of the title compound along with the results of the Hirshfeld surface analysis and the density functional theory (DFT) computational calculations carried out at the B3LYP/6-311 G(d,p) level in order to compare the theoretical and experimentally determined molecular structures in the solid state.



## 2. Structural commentary

The title molecule, (I), adopts a U-shaped conformation with an H20 $\cdots$ C14 separation of 2.83 Å, which is very close to a normal van der Waals contact (2.90 Å). The orientation of the C11–C17 benzyl group is partly determined by an intramolecular C13–H13 $\cdots$ Cg interaction, where Cg is the centroid of the triazole (C9/C10/N3–N5), ring C (Fig. 1 and Table 1). The dihydrobenzodiazole unit is not quite planar, as

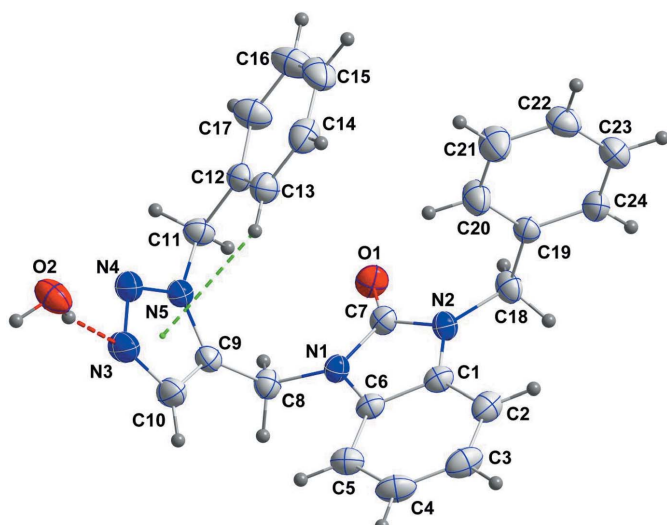


**Figure 1**

The molecular structure of the title compound with the atom-numbering scheme. Displacement ellipsoids are drawn at the 50% probability level. The O–H<sub>UncoordW</sub> $\cdots$ N<sub>Trz</sub> (UncoordW = uncoordinated water, Trz = triazole) hydrogen bond is shown by a red dashed line while the intramolecular C–H $\cdots$  $\pi$ (ring) interaction is depicted by a green dashed line.

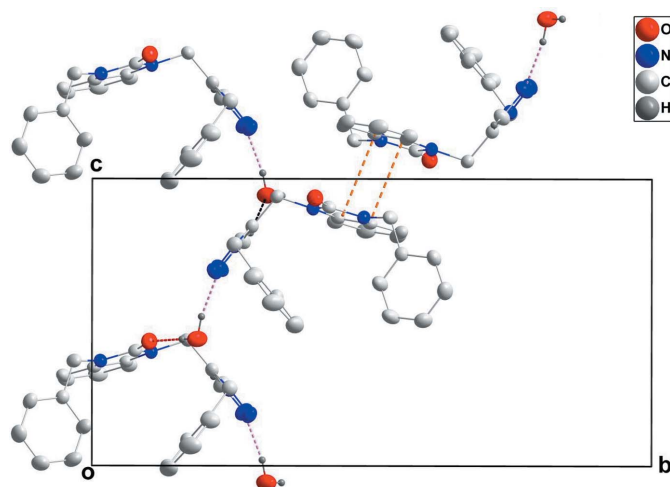


**Figure 2**

A partial packing diagram viewed along the *a*-axis direction with O–H<sub>UncoordW</sub> $\cdots$ O<sub>Dhyr</sub>, O–H<sub>UncoordW</sub> $\cdots$ N<sub>Trz</sub> and C–H<sub>Trz</sub> $\cdots$ O<sub>UncoordW</sub> (UncoordW = uncoordinated water, Dhyr = dihydro, Trz = triazole) hydrogen bonds shown, respectively, as red, pink and black dashed lines. The  $\pi$ -stacking interactions are shown as orange dashed lines.

indicated by the dihedral angle of 2.50 (8) $^\circ$  between the constituent rings *A* (C1–C6) and *B* (N1/N2/C1/C6/C7) and the deviation of atom C7 by 0.0418 (14) Å out of the mean plane through the whole unit. The benzene ring *D* (C12–C17) is inclined to the triazole ring *C* by 78.91 (11) $^\circ$  while the latter ring is inclined to the *B* ring by 64.70 (11) $^\circ$ . The dihedral angle between the mean planes of the *B* and *E* (C19–C24) rings is 87.67 (8) $^\circ$ .

## 3. Supramolecular features

In the crystal, the molecules form chains with the water molecule of crystallization, which extend along [011] through O–H<sub>UncoordW</sub> $\cdots$ O<sub>Dhyr</sub> and O–H<sub>UncoordW</sub> $\cdots$ N<sub>Trz</sub> (UncoordW = uncoordinated water, Dhyr = dihydro, Trz = triazole) hydrogen bonds (Table 1 and Fig. 2). The chains are connected

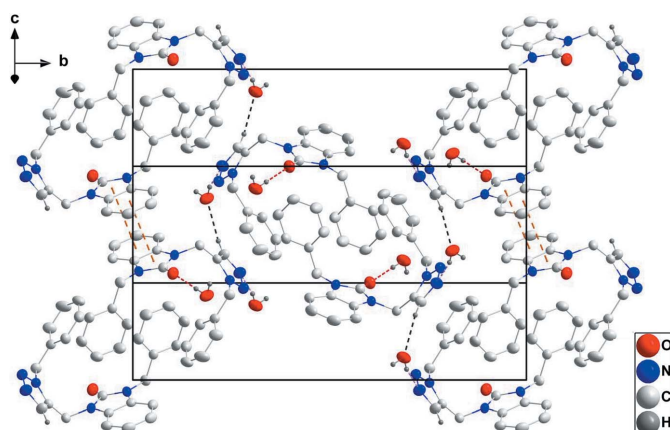


**Figure 3**

A partial packing diagram projected onto (301) with intermolecular interactions depicted as in Fig. 2.

**Table 1**  
Hydrogen-bond geometry ( $\text{\AA}$ ,  $^\circ$ ).

$D-\text{H}\cdots A$	$D-\text{H}$	$\text{H}\cdots A$	$D\cdots A$	$D-\text{H}\cdots A$
$O2-\text{H}2A\cdots N3$	0.87	2.04	2.892 (2)	166
$O2-\text{H}2B\cdots O1^i$	0.87	2.00	2.865 (2)	176
$C10-\text{H}10\cdots O2^y$	0.95	2.48	3.402 (3)	164
$C13-\text{H}13\cdots Cg$	0.95	2.83	3.451 (3)	124

Symmetry codes: (i)  $x - 1, -y + \frac{1}{2}, z - \frac{1}{2}$ ; (v)  $x, -y + \frac{1}{2}, z + \frac{1}{2}$ .

into layers parallel to (010) by  $\text{C}-\text{H}_{\text{Trz}}\cdots \text{O}_{\text{UncoordW}}$  hydrogen bonds (Table 1 and Fig. 2). Intercalation of the dihydrobenzodiazole groups between adjacent layers with concomitant head-to-tail  $\pi$ -stacking interactions between them [ $Cg2\cdots Cg1^i = 3.5694 (11)$   $\text{\AA}$  where  $Cg1$  and  $Cg2$  are the centroids of the  $A$  and  $B$  rings, respectively; symmetry code: (i)  $-x + 1, -y + 1, -z + 2$ ; dihedral angle = 2.50 (10) $^\circ$ ] leads to the final three-dimensional structure (Fig. 3).

#### 4. Hirshfeld surface analysis

In order to visualize the intermolecular interactions in the crystal of the title compound, a Hirshfeld surface (HS) analysis (Hirshfeld, 1977; Spackman & Jayatilaka, 2009) was carried out using *Crystal Explorer 17.5* (Turner *et al.*, 2017). In the HS plotted over  $d_{\text{norm}}$  (Fig. 4), white areas indicate contacts with distances equal to the sum of van der Waals radii, and the red and blue colours indicate distances shorter (in close contact) or longer (distinct contact), respectively, than the van der Waals radii (Venkatesan *et al.*, 2016). The bright-red spots appearing near O1 and hydrogen atom H2B indicate their roles as the respective donors and acceptors. The shape-index of the HS is a tool to visualize the  $\pi$ - $\pi$  stacking by

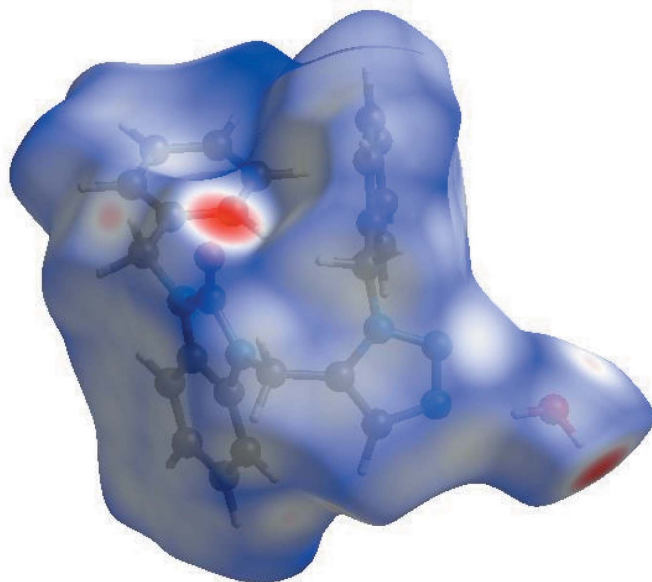


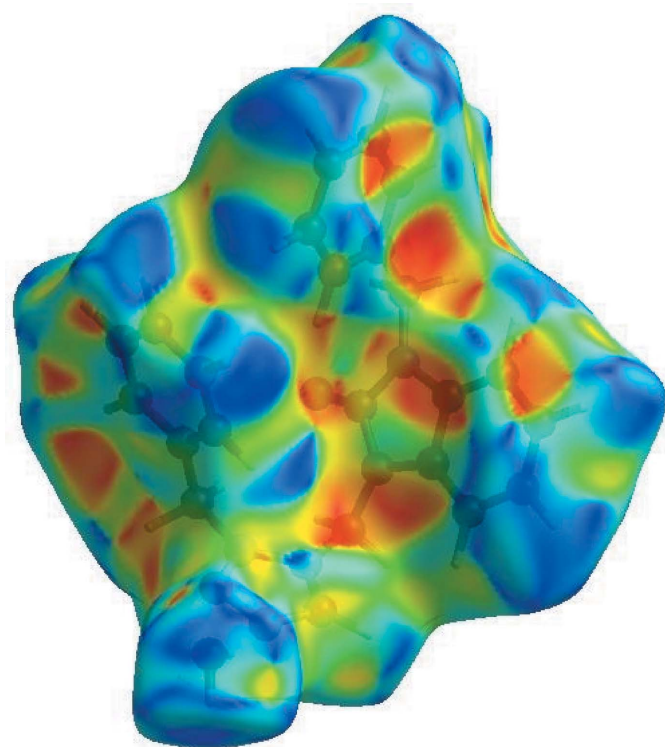
**Figure 4**  
View of the three-dimensional Hirshfeld surface of the title compound plotted over  $d_{\text{norm}}$  in the range  $-0.5603$  to  $1.3285$  a.u.

**Table 2**  
Selected interatomic distances ( $\text{\AA}$ ).

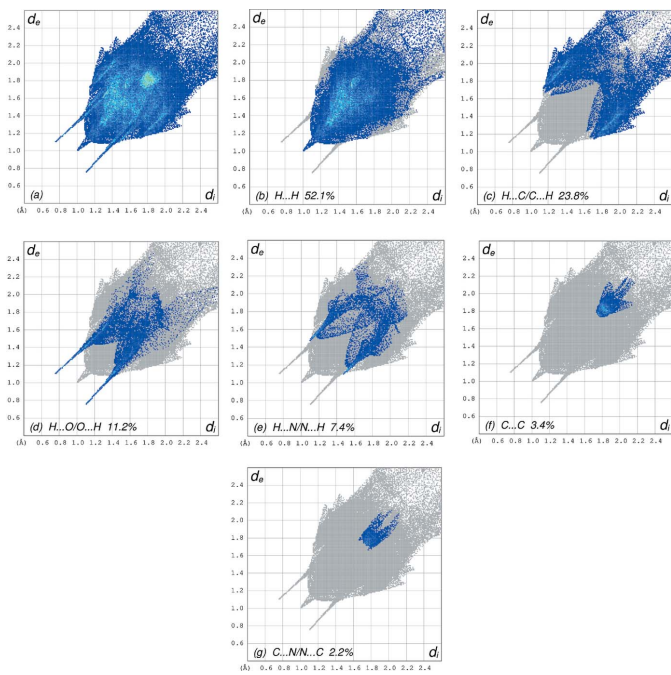
$O2\cdots O1^i$	2.865 (2)	$C10\cdots H5$	2.98
$O2\cdots C17^i$	3.192 (3)	$C11\cdots H8B$	2.90
$O2\cdots N3$	2.892 (2)	$C14\cdots H20$	2.83
$O1\cdots H8B$	2.55	$C18\cdots H2$	2.98
$O1\cdots H11B$	2.81	$C22\cdots H16^{vi}$	2.98
$O1\cdots H18A$	2.56	$C22\cdots H13^{vi}$	2.97
$O1\cdots H18A^{ii}$	2.87	$C23\cdots H16^{vi}$	2.97
$O2\cdots H5^{iii}$	2.64	$H2\cdots N4^{viii}$	2.78
$O2\cdots H11B^i$	2.77	$H2A\cdots N4$	2.62
$O2\cdots H17^i$	2.71	$H2A\cdots N3$	2.04
$N4\cdots C13$	3.200 (3)	$H2B\cdots O1^i$	2.00
$N2\cdots H20$	2.60	$H2B\cdots H11B^i$	2.48
$N4\cdots H13$	2.73	$H3\cdots H15^{vi}$	2.48
$N5\cdots H13$	2.52	$H4\cdots H18A^{ix}$	2.57
$C1\cdots C20$	3.557 (3)	$H5\cdots H10$	2.44
$C2\cdots C6^{iv}$	3.542 (3)	$H8A\cdots N4^v$	2.67
$C3\cdots C7^{iv}$	3.540 (3)	$H8B\cdots H11B$	2.27
$C5\cdots C9$	3.592 (3)	$H10\cdots O2^v$	2.48
$C9\cdots C5$	3.592 (3)	$H10\cdots H17^{ix}$	2.46
$C10\cdots O2^v$	3.402 (3)	$H11A\cdots C15^v$	2.92
$C11\cdots C15^v$	3.421 (3)	$H11A\cdots H17$	2.51
$C14\cdots C20$	3.505 (3)	$H16\cdots H23^{vii}$	2.44
$C2\cdots H18B$	2.98	$H16\cdots H22^{vii}$	2.46
$C3\cdots H15^{vi}$	2.88	$H18A\cdots H18A^{ii}$	2.19
$C8\cdots H11B$	2.79	$H18B\cdots H24$	2.43
$C8\cdots H5$	2.99	$H24\cdots N3^{viii}$	2.76

Symmetry codes: (i)  $x - 1, -y + \frac{1}{2}, z - \frac{1}{2}$ ; (ii)  $-x + 2, -y + 1, -z + 2$ ; (iii)  $x, -y + \frac{1}{2}, z - \frac{1}{2}$ ; (iv)  $-x + 1, -y + 1, -z + 2$ ; (v)  $x, -y + \frac{1}{2}, z + \frac{1}{2}$ ; (vi)

the presence of adjacent red and blue triangles; if there are no adjacent red and/or blue triangles, then there are no  $\pi$ - $\pi$  interactions. Fig. 5 clearly suggests that there are  $\pi$ - $\pi$  interactions in (I).



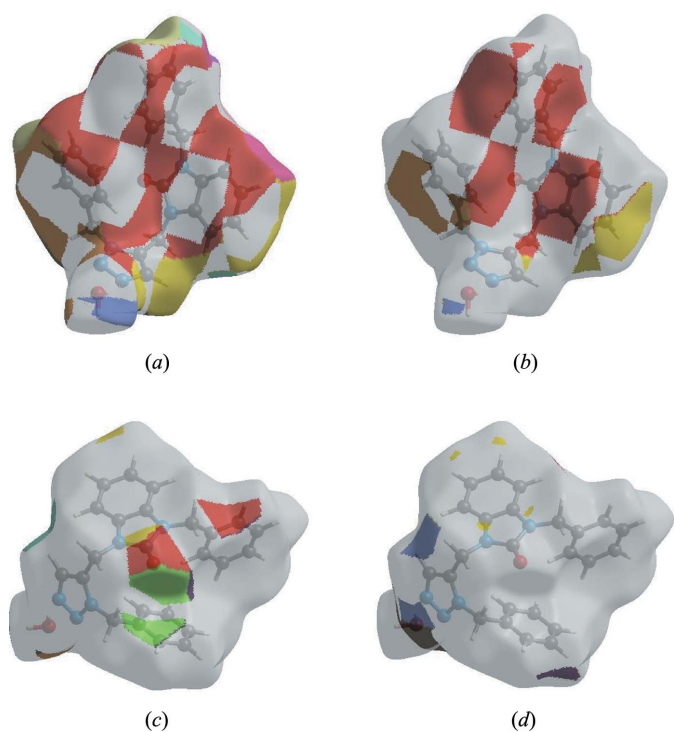
**Figure 5**  
Hirshfeld surface of the title compound plotted over shape-index.

**Figure 6**

The full two-dimensional fingerprint plots for the title compound, showing (a) all interactions, and delineated into (b)  $\text{H}\cdots\text{H}$ , (c)  $\text{H}\cdots\text{C}/\text{C}\cdots\text{H}$ , (d)  $\text{H}\cdots\text{O}/\text{O}\cdots\text{H}$ , (e)  $\text{H}\cdots\text{N}/\text{N}\cdots\text{H}$ , (f)  $\text{C}\cdots\text{C}$  and (g)  $\text{C}\cdots\text{N}/\text{N}\cdots\text{C}$  interactions. The  $d_i$  and  $d_e$  values are the closest internal and external distances (in Å) from given points on the Hirshfeld surface contacts.

The overall two-dimensional fingerprint plot, Fig. 6a, and those delineated into  $\text{H}\cdots\text{H}$ ,  $\text{H}\cdots\text{C}/\text{C}\cdots\text{H}$ ,  $\text{H}\cdots\text{O}/\text{O}\cdots\text{H}$ ,  $\text{H}\cdots\text{N}/\text{N}\cdots\text{H}$ ,  $\text{C}\cdots\text{C}$  and  $\text{C}\cdots\text{N}/\text{N}\cdots\text{C}$  contacts (McKinnon *et al.*, 2007) are illustrated in Fig. 6b–g, respectively, together with their relative contributions to the Hirshfeld surface. The most important interaction (Table 2) is  $\text{H}\cdots\text{H}$ , contributing 52.1% to the overall crystal packing, which is reflected in Fig. 6b as widely scattered points of high density due to the large hydrogen content of the molecule with the tip at  $d_e = d_i = 1.00$  Å. The presence of  $\text{C}-\text{H}\cdots\pi$  interactions give rise to pairs of characteristic wings in the fingerprint plot delineated into  $\text{H}\cdots\text{C}/\text{C}\cdots\text{H}$  contacts (23.8% contribution to the HS), Fig. 6c, (Table 2) with triple pairs of spikes with the tips at  $d_e + d_i = 2.86$ , 2.82 and 2.85 Å. The scattered points in the pair of wings in the fingerprint plots delineated into  $\text{H}\cdots\text{O}/\text{O}\cdots\text{H}$  contacts (11.2% contribution), Fig. 6d, have a symmetrical distribution with the edges at  $d_e + d_i = 1.85$  Å. The  $\text{H}\cdots\text{N}/\text{N}\cdots\text{H}$  contacts, contributing 7.4% to the overall crystal packing, are shown in Fig. 6e as widely scattered points with the tips at  $d_e + d_i = 2.56$  Å. The  $\text{C}\cdots\text{C}$  contacts, Fig. 6f, have an arrow-shaped distribution of points with the tip at  $d_e = d_i = 1.77$  Å. Finally, the  $\text{C}\cdots\text{N}/\text{N}\cdots\text{C}$  interactions (2.2%) are reflected in Fig. 6g as tiny characteristic wings with the tips at  $d_e + d_i = 3.44$  Å.

The Hirshfeld surface representations with the function  $d_{\text{norm}}$  plotted onto the surface are shown for the  $\text{H}\cdots\text{H}$ ,  $\text{H}\cdots\text{C}/\text{C}\cdots\text{H}$ ,  $\text{H}\cdots\text{O}/\text{O}\cdots\text{H}$  and  $\text{H}\cdots\text{N}/\text{N}\cdots\text{H}$  interactions in Fig. 7a–d, respectively.

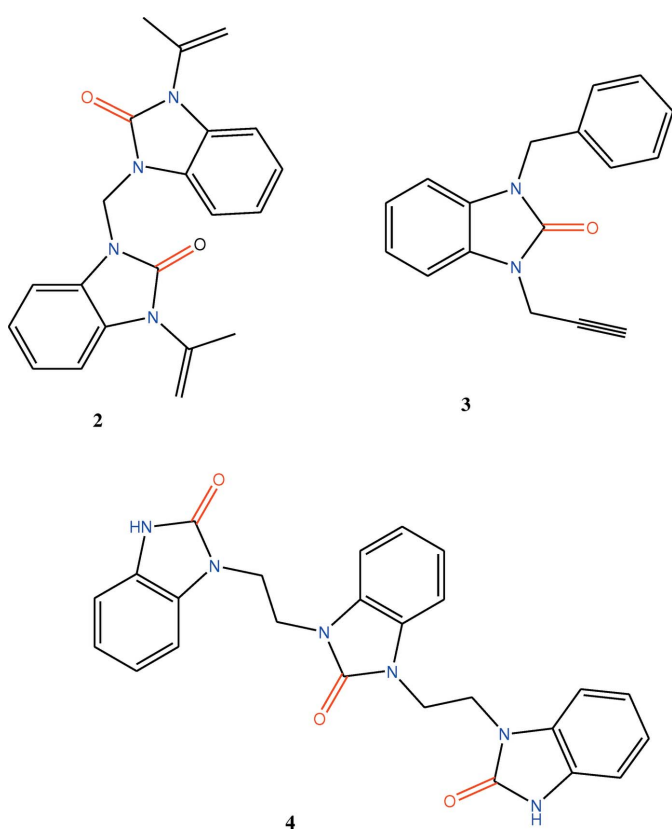
**Figure 7**

The Hirshfeld surface representations with the function  $d_{\text{norm}}$  plotted onto the surface for (a)  $\text{H}\cdots\text{H}$ , (b)  $\text{H}\cdots\text{C}/\text{C}\cdots\text{H}$ , (c)  $\text{H}\cdots\text{O}/\text{O}\cdots\text{H}$  and (d)  $\text{H}\cdots\text{N}/\text{N}\cdots\text{H}$  interactions.

The Hirshfeld surface analysis confirms the importance of H-atom contacts in establishing the packing. The large number of  $\text{H}\cdots\text{H}$ ,  $\text{H}\cdots\text{C}/\text{C}\cdots\text{H}$  and  $\text{H}\cdots\text{O}/\text{O}\cdots\text{H}$  interactions suggest that van der Waals interactions and hydrogen bonding play the major roles in the crystal packing (Hathwar *et al.*, 2015).

## 5. Database survey

An N-substituted benzoimidazol-2-one analogue (Saber *et al.*, 2018a,b; Saber *et al.*, 2020) and other similar compounds have also been reported (Belaziz *et al.*, 2012, 2013; Bouayad *et al.*, 2015). In derivatives of benzimidazolin-2-one in which both nitrogen atoms form exocyclic C–N bonds, the bicyclic ring system is either planar, has a slight twist end-to-end, or, in the cases where the exocyclic substituents form a ring, has a very shallow bowl shape. The closest examples to the title compound are **2** (Saber *et al.*, 2018a) and **3** (Saber *et al.*, 2018b) with **4** (Díez-Barra *et al.*, 1997) as a more distant relative. In **3**, the C–N bond, connecting the nitrogen atoms to form exocyclic units are 1.4632 (15) and 1.4525 (16) Å, while in the title compound, the C–N bonds are 1.4301 (15) and 1.4525 (16) Å. In the bicyclic units, they are in an *anti*-arrangement, and this is basically the same for **2**. Interestingly, the three bicyclic units in **4** are close to all being *syn* to one another.



## 6. DFT calculations

The optimized structure of the title compound, (I), in the gas phase was generated theoretically *via* density functional theory (DFT) using standard B3LYP functional and 6-311 G(d,p) basis-set calculations (Becke, 1993) as implemented in *GAUSSIAN 09* (Frisch *et al.*, 2009). The theoretical and experimental results are in good agreement (Table 3). The highest-occupied molecular orbital (HOMO), acting as an electron donor, and the lowest-unoccupied molecular orbital (LUMO), acting as an electron acceptor, are very important parameters for quantum chemistry. When the energy gap is small, the molecule is highly polarizable and has high chemical reactivity. The DFT calculations provide some important information on the reactivity and site selectivity of the molecular framework.  $E_{\text{HOMO}}$  and  $E_{\text{LUMO}}$  clarify the inevitable charge-exchange collaboration inside the studied material, electronegativity ( $\chi$ ), hardness ( $\eta$ ), potential ( $\mu$ ), electrophilicity ( $\omega$ ) and softness ( $\sigma$ ) are recorded in Table 4. The significance of  $\eta$  and  $\sigma$  is to evaluate both the reactivity and stability. The electron transition from the HOMO to the LUMO energy level is shown in Fig. 8. The HOMO and LUMO are localized in the plane extending over the whole 1-benzyl-3-[{(1-benzyl-1*H*-1,2,3-triazol-4-yl)methyl]-2,3-dihydro-1*H*-1,3-benzodiazol-2-one hydrate ring. The energy band gap [ $\Delta E = E_{\text{LUMO}} - E_{\text{HOMO}}$ ] of the molecule is 5.3468 eV, and the frontier molecular orbital energies,  $E_{\text{HOMO}}$  and  $E_{\text{LUMO}}$  are  $-6.1633$  and  $-0.8166$  eV, respectively.

**Table 3**  
Comparison of selected (X-ray and DFT) geometric data (Å, °).

Bonds/angles	X-ray	B3LYP/6-311G(d,p)
O1—C7	1.225 (2)	1.25497
N1—C7	1.384 (2)	1.40076
N1—C6	1.397 (2)	1.40603
N1—C8	1.452 (2)	1.46502
N2—C7	1.379 (2)	1.39180
N2—C1	1.395 (2)	1.40574
N2—C18	1.450 (2)	1.47028
N3—N4	1.314 (2)	1.32954
N3—C10	1.358 (3)	1.37406
N4—N5	1.347 (2)	1.38781
N5—C9	1.356 (2)	1.37548
N5—C11	1.452 (2)	1.47090
C7—N1—C6	109.72 (15)	109.64541
C7—N1—C8	123.68 (15)	122.59694
C6—N1—C8	125.96 (15)	127.83740
C7—N2—C1	109.90 (15)	109.86320
C7—N2—C18	123.91 (16)	122.77835
C1—N2—C18	125.82 (16)	128.23580
N4—N3—C10	108.55 (17)	108.75382
N3—N4—N5	107.17 (16)	107.07997
N4—N5—C9	111.14 (15)	110.25168
N4—N5—C11	118.44 (16)	118.90455

## 7. Synthesis and crystallization

To a mixture of 3-methyl-1-(prop-2-ynyl)-3,4-dihydroquinoxalin-2(1*H*)-one (0.65 mmol) in ethanol (20 ml) was added 1-(azidomethyl)benzene (1.04 mmol). The mixture was stirred under reflux for 24 h. After completion of the reaction (monitored by TLC), the solution was concentrated and the residue obtained was purified by column chromatography on silica gel by using as eluent a mixture (hexane/ethyl acetate: 9/

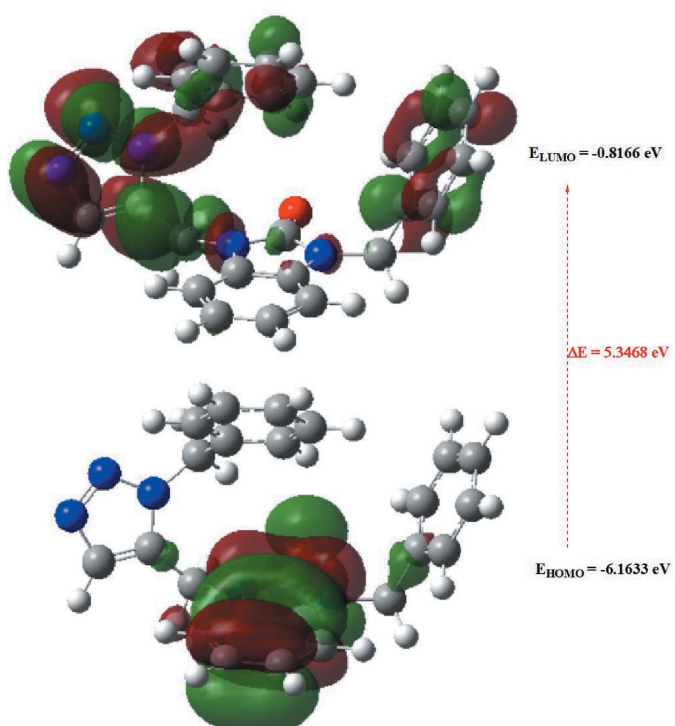


**Figure 8**  
The energy band gap of the title compound, (I).

**Table 4**  
Calculated energies.

Molecular Energy (a.u.) (eV)	Compound (I)
Total Energy, <i>TE</i> (eV)	-34723.0011
$E_{\text{HOMO}}$ (eV)	-6.1633
$E_{\text{LUMO}}$ (eV)	-0.8166
Gap $\Delta E$ (eV)	5.3468
Dipole moment, $\mu$ (Debye)	5.5500
Ionization potential <i>I</i> (eV)	6.1633
Electron affinity, <i>A</i>	0.8166
Electronegativity, $\chi$	3.4900
Hardness, $\eta$	2.6734
Electrophilicity index, $\omega$	2.2780
Softness, $\sigma$	0.3741
Fraction of electron transferred, $\Delta N$	0.6565

1). The isolated solid product was recrystallized from ethanol to afford yellow crystals (yield: in 19%).

## 8. Refinement

The experimental details including the crystal data, data collection and refinement are summarized in Table 5. Hydrogen atoms were included as riding contributions in idealized positions with C—H = 0.95–0.99 Å and  $U_{\text{iso}}(\text{H}) = 1.2U_{\text{eq}}(\text{C})$ .

## Funding information

The support of NSF-MRI grant No. 1228232 for the purchase of the diffractometer and Tulane University for support of the Tulane Crystallography Laboratory are gratefully acknowledged. TH is grateful to Hacettepe University Scientific Research Project Unit (grant No. 013 D04 602 004).

## References

<b>Table 5</b> Experimental details.	
Crystal data	
Chemical formula	$C_{24}H_{21}N_5O \cdot H_2O$
$M_r$	413.47
Crystal system, space group	Monoclinic, $P2_1/c$
Temperature (K)	150
$a, b, c$ (Å)	9.0872 (2), 21.1012 (4), 11.7134 (2)
$\beta$ (°)	112.654 (1)
$V$ (Å <sup>3</sup> )	2072.77 (7)
$Z$	4
Radiation type	Cu $K\alpha$
$\mu$ (mm <sup>-1</sup> )	0.70
Crystal size (mm)	0.18 × 0.08 × 0.01
Data collection	
Diffractometer	Bruker D8 VENTURE PHOTON 100 CMOS
Absorption correction	Multi-scan ( <i>SADABS</i> ; Krause <i>et al.</i> , 2015)
$T_{\min}, T_{\max}$	0.85, 0.99
No. of measured, independent and observed [ $I > 2\sigma(I)$ ] reflections	15080, 3887, 2909
$R_{\text{int}}$	0.057
(sin $\theta/\lambda$ ) <sub>max</sub> (Å <sup>-1</sup> )	0.610
Refinement	
$R[F^2 > 2\sigma(F^2)], wR(F^2), S$	0.048, 0.113, 1.06
No. of reflections	3887
No. of parameters	280
H-atom treatment	H-atom parameters constrained
$\Delta\rho_{\text{max}}, \Delta\rho_{\text{min}}$ (e Å <sup>-3</sup> )	0.22, -0.22
Computer programs: <i>APEX3</i> and <i>SAINT</i> (Bruker, 2016), <i>SHELXT2014</i> (Sheldrick, 2015a), <i>SHELXL2018</i> (Sheldrick, 2015b) and <i>DIAMOND</i> (Brandenburg & Putz, 2012).	
M., Knox, J. E., Cross, J. B., Bakken, V., Adamo, C., Jaramillo, J., Gomperts, R., Stratmann, R. E., Yazyev, O., Austin, A. J., Cammi, R., Pomelli, C., Ochterski, J. W., Martin, R. L., Morokuma, K., Zakrzewski, V. G., Voth, G. A., Salvador, P., Dannenberg, J. J., Dapprich, S., Daniels, A. D., Farkas, ., Foresman, J. B., Ortiz, J. V., Cioslowski, J. & Fox, D. J. (2009). <i>GAUSSIAN 09</i> . Gaussian Inc., Wallingford, CT, US	
Gaba, M., Singh, S. & Mohan, C. (2014). <i>Eur. J. Med. Chem.</i> <b>76</b> , 494–505.	
Garuti, L., Roberti, M., Malagoli, M., Rossi, T. & Castelli, M. (2000). <i>Bioorg. Med. Chem. Lett.</i> <b>10</b> , 2193–2195.	
Hathwar, V. R., Sist, M., Jørgensen, M. R. V., Mamakhe, A. H., Wang, X., Hoffmann, C. M., Sugimoto, K., Overgaard, J. & Iversen, B. B. (2015). <i>IUCrJ</i> , <b>2</b> , 563–574.	
Hirshfeld, F. L. (1977). <i>Theor. Chim. Acta</i> , <b>44</b> , 129–138.	
Krause, L., Herbst-Irmer, R., Sheldrick, G. M. & Stalke, D. (2015). <i>J. Appl. Cryst.</i> <b>48</b> , 3–10.	
Lakhrissi, B., Benksim, A., Massouli, M., Essassi, el M., Lequart, V., Joly, N., Beaupère, D., Wadouachi, A. & Martin, P. (2008). <i>Carbohydr. Res.</i> <b>343</b> , 421–433.	
Mavrova, A., Ts, Denkova, P., Tsenov, Y. A., Anichina, K. K. & Vutchev, D. I. (2007). <i>Bioorg. Med. Chem.</i> <b>15</b> , 6291–6297.	
McKinnon, J. J., Jayatilaka, D. & Spackman, M. A. (2007). <i>Chem. Commun.</i> pp. 3814–3816.	
Mondieig, D., Lakhrissi, L., El Assyry, A., Lakhrissi, B., Negrier, P., Essassi, E. M., Massouli, M., Michel Leger, J. & Benali, B. (2013). <i>J. Mar. Chim. Heterocycl.</i> <b>12</b> , 51–61.	
Navarrete-Vazquez, G., Cedillo, R., Hernandez-Campos, A., Yepez, L., Hernandez-Luis, F., Valdez, J., Morales, R., Cortes, R., Hernandez, M. & Castillo, R. (2001). <i>Bioorg Med Chem.</i> <b>11</b> , 187–190.	
Olesen, S. P., Munch, E., Moldt, P. & Drejer, J. (1994). <i>Eur. J. Pharmacol.</i> <b>251</b> , 53–59.	

- Ouzidan, Y., Kandri Rodi, Y., Fronczek, F. R., Venkatraman, R., El Ammari, L. & Essassi, E. M. (2011). *Acta Cryst. E* **67**, o362–o363.
- Rao, A., Chimirri, A., De Clercq, E., Monforte, A. M., Monforte, P., Pannecouque, C. & Zappalà, M. (2002). *Farmaco*, **57**, 819–823.
- Ravina, E., Sanchez-Alonso, R., Fueyo, J., Baltar, M. P., Bos, J., Iglesias, R. & Sanmartin, M. L. (1993). *Arzneim. Forsch.* **43**, 684–694.
- Rémond, G., Portevin, B., Bonnet, J., Canet, E., Regoli, D. & De Nanteuil, G. (1997). *Eur. J. Med. Chem.* **32**, 843–868.
- Saber, A., Sebbar, N. K., Hökelek, T., El hafi, M., Mague, J. T. & Essassi, E. M. (2018b). *Acta Cryst. E* **74**, 1842–1846.
- Saber, A., Sebbar, N. K., Hökelek, T., Hni, B., Mague, J. T. & Essassi, E. M. (2018a). *Acta Cryst. E* **74**, 1746–1750.
- Saber, A., Sebbar, N. K., Sert, Y., Alzaqri, N., Hökelek, T., El Ghayati, L., Talbaoui, A., Mague, J. T., Baba, Y. F., Urrutigoity, M. & Essassi, M. (2020). *J. Mol. Struct.* **1200**, 127174.
- Sebbar, N. K., Mekhzoum, M. E. M., Essassi, E. M., Abdelfettah Z., Ouzidan Y., Kandri, Rodi Y., Talbaoui, A. & Bakri, Y. (2016). *J. Mar. Chim. Heterocycl.* **15**, 1–11.
- Serafin, B., Borkowska, G., Glowczyk, J., Kowalska, I. & Rump, S. (1989). *Pol. J. Pharmcol. Pharm.* **41**, 89–96.
- Sheldrick, G. M. (2015a). *Acta Cryst. A* **71**, 3–8.
- Sheldrick, G. M. (2015b). *Acta Cryst. C* **71**, 3–8.
- Spackman, M. A. & Jayatilaka, D. (2009). *CrystEngComm*, **11**, 19–32.
- Thakurdesai, P. A., Wadodkar, S. G. & Chopade, C. T. (2007). *Pharmacology Online* **1**, 314–329.
- Turner, M. J., McKinnon, J. J., Wolff, S. K., Grimwood, D. J., Spackman, P. R., Jayatilaka, D. & Spackman, M. A. (2017). *Crystal Explorer 17*. The University of Western Australia.
- Venkatesan, P., Thamotharan, S., Ilangovan, A., Liang, H. & Sundius, T. (2016). *Spectrochim. Acta Part A*, **153**, 625–636.

# supporting information

*Acta Cryst.* (2020). E76, 95-101 [https://doi.org/10.1107/S2056989019016876]

## Crystal structure, Hirshfeld surface analysis and DFT studies of 1-benzyl-3-[(1-benzyl-1*H*-1,2,3-triazol-5-yl)methyl]-2,3-dihydro-1*H*-1,3-benzodiazol-2-one monohydrate

**Asmaa Saber, Nada Kheira Sebbar, Tuncer Hökelek, Mohamed Labd Taha, Joel T. Mague, Noureddine Hamou Ahabchane and El Mokhtar Essassi**

### Computing details

Data collection: *APEX3* (Bruker, 2016); cell refinement: *SAINT* (Bruker, 2016); data reduction: *SAINT* (Bruker, 2016); program(s) used to solve structure: *SHELXT2014* (Sheldrick, 2015a); program(s) used to refine structure: *SHELXL2018* (Sheldrick, 2015b); molecular graphics: *DIAMOND* (Brandenburg & Putz, 2012); software used to prepare material for publication: *SHELXL2018* (Sheldrick, 2015b).

### 1-Benzyl-3-[(1-benzyl-1*H*-1,2,3-triazol-5-yl)methyl]-2,3-dihydro-1*H*-1,3-benzodiazol-2-one monohydrate

#### Crystal data

$C_{24}H_{21}N_5O \cdot H_2O$   
 $M_r = 413.47$   
Monoclinic,  $P2_1/c$   
 $a = 9.0872 (2)$  Å  
 $b = 21.1012 (4)$  Å  
 $c = 11.7134 (2)$  Å  
 $\beta = 112.654 (1)^\circ$   
 $V = 2072.77 (7)$  Å<sup>3</sup>  
 $Z = 4$

$F(000) = 872$   
 $D_x = 1.325$  Mg m<sup>-3</sup>  
Cu  $K\alpha$  radiation,  $\lambda = 1.54178$  Å  
Cell parameters from 9060 reflections  
 $\theta = 4.2\text{--}70.2^\circ$   
 $\mu = 0.70$  mm<sup>-1</sup>  
 $T = 150$  K  
Plate, colourless  
0.18 × 0.08 × 0.01 mm

#### Data collection

Bruker D8 VENTURE PHOTON 100 CMOS  
diffractometer  
Radiation source: INCOATEC I $\mu$ S micro-focus  
source  
Mirror monochromator  
Detector resolution: 10.4167 pixels mm<sup>-1</sup>  
 $\omega$  scans  
Absorption correction: multi-scan  
(SADABS; Krause *et al.*, 2015)

$T_{\min} = 0.85, T_{\max} = 0.99$   
15080 measured reflections  
3887 independent reflections  
2909 reflections with  $I > 2\sigma(I)$   
 $R_{\text{int}} = 0.057$   
 $\theta_{\max} = 70.2^\circ, \theta_{\min} = 4.2^\circ$   
 $h = -11 \rightarrow 10$   
 $k = -24 \rightarrow 25$   
 $l = -14 \rightarrow 13$

#### Refinement

Refinement on  $F^2$   
Least-squares matrix: full  
 $R[F^2 > 2\sigma(F^2)] = 0.048$   
 $wR(F^2) = 0.113$   
 $S = 1.06$

3887 reflections  
280 parameters  
0 restraints  
Primary atom site location: structure-invariant  
direct methods

Secondary atom site location: difference Fourier map

Hydrogen site location: mixed  
H-atom parameters constrained

$$w = 1/[\sigma^2(F_o^2) + (0.0367P)^2 + 0.901P]$$

where  $P = (F_o^2 + 2F_c^2)/3$

$$(\Delta/\sigma)_{\max} < 0.001$$

$$\Delta\rho_{\max} = 0.22 \text{ e } \text{\AA}^{-3}$$

$$\Delta\rho_{\min} = -0.21 \text{ e } \text{\AA}^{-3}$$

### Special details

**Geometry.** All esds (except the esd in the dihedral angle between two l.s. planes) are estimated using the full covariance matrix. The cell esds are taken into account individually in the estimation of esds in distances, angles and torsion angles; correlations between esds in cell parameters are only used when they are defined by crystal symmetry. An approximate (isotropic) treatment of cell esds is used for estimating esds involving l.s. planes.

**Refinement.** Refinement of  $F^2$  against ALL reflections. The weighted R-factor wR and goodness of fit S are based on  $F^2$ , conventional R-factors R are based on F, with F set to zero for negative  $F^2$ . The threshold expression of  $F^2 > 2\text{sigma}(F^2)$  is used only for calculating R-factors(gt) etc. and is not relevant to the choice of reflections for refinement. R-factors based on  $F^2$  are statistically about twice as large as those based on F, and R-factors based on ALL data will be even larger. H-atoms attached to carbon were placed in calculated positions ( $\text{C}-\text{H} = 0.95 - 0.99 \text{ \AA}$ ) while those attached to oxygen were placed in locations derived from a difference map and their coordinates adjusted to give  $\text{O}-\text{H} = 0.87 \text{ \AA}$ . All were included as riding contributions with isotropic displacement parameters 1.2 - 1.5 times those of the attached atoms.

### Fractional atomic coordinates and isotropic or equivalent isotropic displacement parameters ( $\text{\AA}^2$ )

	x	y	z	$U_{\text{iso}}^*/U_{\text{eq}}$
O1	0.85567 (15)	0.39779 (7)	0.93327 (13)	0.0375 (4)
N1	0.58475 (17)	0.39409 (7)	0.89638 (14)	0.0267 (3)
N2	0.68572 (18)	0.48484 (7)	0.86568 (14)	0.0278 (3)
N3	0.3094 (2)	0.22818 (9)	0.68794 (17)	0.0426 (5)
N4	0.4467 (2)	0.21861 (8)	0.67770 (16)	0.0378 (4)
N5	0.55663 (19)	0.25352 (8)	0.76599 (15)	0.0300 (4)
C1	0.5258 (2)	0.49606 (9)	0.84381 (16)	0.0274 (4)
C2	0.4364 (2)	0.55101 (10)	0.81370 (18)	0.0350 (5)
H2	0.480398	0.590041	0.801540	0.042*
C3	0.2785 (3)	0.54622 (11)	0.80211 (19)	0.0411 (5)
H3	0.213195	0.583008	0.781973	0.049*
C4	0.2141 (2)	0.48927 (12)	0.8192 (2)	0.0416 (5)
H4	0.105243	0.487817	0.808961	0.050*
C5	0.3051 (2)	0.43389 (11)	0.85099 (18)	0.0342 (5)
H5	0.261424	0.394902	0.863712	0.041*
C6	0.4618 (2)	0.43874 (9)	0.86300 (16)	0.0263 (4)
C7	0.7242 (2)	0.42276 (9)	0.90173 (17)	0.0275 (4)
C8	0.5772 (2)	0.32986 (9)	0.93828 (18)	0.0307 (4)
H8A	0.523147	0.330364	0.997257	0.037*
H8B	0.686995	0.313896	0.982830	0.037*
C9	0.4903 (2)	0.28571 (9)	0.83436 (17)	0.0288 (4)
C10	0.3330 (2)	0.26854 (10)	0.7837 (2)	0.0381 (5)
H10	0.252957	0.282630	0.811211	0.046*
C11	0.7188 (2)	0.25400 (10)	0.77111 (19)	0.0337 (5)
H11A	0.752881	0.209810	0.766704	0.040*
H11B	0.790188	0.271831	0.851613	0.040*
C12	0.7378 (2)	0.29187 (9)	0.66852 (17)	0.0303 (4)
C13	0.6180 (3)	0.32884 (10)	0.58683 (19)	0.0372 (5)

H13	0.516342	0.330255	0.592204	0.045*
C14	0.6458 (3)	0.36398 (11)	0.4968 (2)	0.0439 (5)
H14	0.562951	0.389101	0.440157	0.053*
C15	0.7931 (3)	0.36233 (12)	0.4897 (2)	0.0499 (6)
H15	0.813571	0.387548	0.430265	0.060*
C16	0.9119 (3)	0.32390 (14)	0.5694 (2)	0.0531 (7)
H16	1.012885	0.321923	0.563017	0.064*
C17	0.8840 (3)	0.28853 (12)	0.6578 (2)	0.0439 (6)
H17	0.965324	0.261779	0.711555	0.053*
C18	0.8011 (2)	0.53227 (10)	0.86554 (18)	0.0336 (5)
H18A	0.909556	0.515338	0.911413	0.040*
H18B	0.787800	0.570113	0.910627	0.040*
C19	0.7883 (2)	0.55247 (9)	0.73841 (17)	0.0280 (4)
C20	0.7223 (3)	0.51411 (11)	0.6354 (2)	0.0435 (5)
H20	0.679963	0.473924	0.643246	0.052*
C21	0.7171 (3)	0.53360 (12)	0.5208 (2)	0.0493 (6)
H21	0.671787	0.506684	0.450937	0.059*
C22	0.7773 (3)	0.59167 (12)	0.5081 (2)	0.0430 (5)
H22	0.772714	0.605182	0.429394	0.052*
C23	0.8446 (3)	0.63033 (11)	0.6103 (2)	0.0432 (5)
H23	0.886487	0.670536	0.602007	0.052*
C24	0.8509 (2)	0.61052 (10)	0.7246 (2)	0.0357 (5)
H24	0.898875	0.637078	0.794666	0.043*
O2	0.10404 (17)	0.18802 (8)	0.44186 (14)	0.0478 (4)
H2A	0.155922	0.195519	0.520249	0.072*
H2B	0.031707	0.160858	0.441258	0.072*

Atomic displacement parameters ( $\text{\AA}^2$ )

	$U^{11}$	$U^{22}$	$U^{33}$	$U^{12}$	$U^{13}$	$U^{23}$
O1	0.0242 (7)	0.0395 (9)	0.0441 (8)	0.0055 (6)	0.0078 (6)	-0.0002 (7)
N1	0.0247 (8)	0.0244 (8)	0.0286 (8)	0.0013 (6)	0.0077 (6)	-0.0006 (6)
N2	0.0259 (8)	0.0263 (9)	0.0283 (8)	-0.0016 (7)	0.0072 (6)	0.0013 (7)
N3	0.0363 (9)	0.0486 (12)	0.0454 (11)	-0.0144 (9)	0.0184 (8)	-0.0126 (9)
N4	0.0385 (9)	0.0358 (10)	0.0409 (10)	-0.0099 (8)	0.0174 (8)	-0.0081 (8)
N5	0.0306 (8)	0.0291 (9)	0.0316 (9)	-0.0037 (7)	0.0132 (7)	-0.0018 (7)
C1	0.0267 (9)	0.0319 (11)	0.0206 (9)	0.0029 (8)	0.0059 (7)	-0.0007 (7)
C2	0.0430 (11)	0.0328 (12)	0.0277 (10)	0.0085 (9)	0.0120 (9)	0.0036 (8)
C3	0.0438 (12)	0.0442 (14)	0.0339 (11)	0.0195 (10)	0.0134 (9)	0.0054 (9)
C4	0.0303 (10)	0.0591 (15)	0.0360 (12)	0.0118 (10)	0.0132 (9)	0.0009 (10)
C5	0.0302 (10)	0.0429 (13)	0.0311 (10)	0.0015 (9)	0.0135 (8)	-0.0007 (9)
C6	0.0255 (9)	0.0303 (11)	0.0215 (9)	0.0024 (8)	0.0071 (7)	-0.0011 (8)
C7	0.0232 (9)	0.0302 (10)	0.0252 (9)	-0.0006 (8)	0.0050 (7)	-0.0023 (8)
C8	0.0345 (10)	0.0279 (11)	0.0280 (10)	0.0011 (8)	0.0101 (8)	0.0026 (8)
C9	0.0309 (9)	0.0272 (10)	0.0297 (10)	-0.0018 (8)	0.0132 (8)	0.0019 (8)
C10	0.0350 (11)	0.0409 (13)	0.0416 (12)	-0.0073 (9)	0.0182 (9)	-0.0083 (10)
C11	0.0288 (10)	0.0375 (12)	0.0362 (11)	0.0025 (9)	0.0138 (8)	0.0018 (9)
C12	0.0303 (10)	0.0318 (11)	0.0283 (10)	-0.0052 (8)	0.0108 (8)	-0.0047 (8)

C13	0.0401 (11)	0.0333 (12)	0.0401 (12)	0.0026 (9)	0.0177 (9)	0.0022 (9)
C14	0.0584 (14)	0.0363 (13)	0.0350 (12)	0.0035 (11)	0.0159 (10)	0.0016 (9)
C15	0.0679 (16)	0.0510 (15)	0.0377 (13)	-0.0150 (13)	0.0279 (12)	-0.0003 (11)
C16	0.0404 (12)	0.0785 (19)	0.0447 (14)	-0.0136 (13)	0.0211 (11)	0.0002 (13)
C17	0.0313 (10)	0.0601 (16)	0.0386 (12)	-0.0021 (10)	0.0115 (9)	0.0025 (11)
C18	0.0328 (10)	0.0340 (11)	0.0296 (10)	-0.0092 (9)	0.0070 (8)	-0.0023 (9)
C19	0.0240 (9)	0.0285 (10)	0.0309 (10)	-0.0005 (8)	0.0099 (7)	-0.0008 (8)
C20	0.0551 (14)	0.0388 (13)	0.0352 (12)	-0.0153 (11)	0.0159 (10)	-0.0061 (10)
C21	0.0625 (15)	0.0503 (15)	0.0340 (12)	-0.0167 (12)	0.0173 (11)	-0.0101 (11)
C22	0.0454 (12)	0.0512 (15)	0.0351 (12)	-0.0047 (11)	0.0188 (10)	0.0023 (10)
C23	0.0494 (13)	0.0384 (13)	0.0491 (13)	-0.0075 (10)	0.0272 (11)	0.0008 (10)
C24	0.0376 (11)	0.0323 (11)	0.0393 (12)	-0.0052 (9)	0.0171 (9)	-0.0062 (9)
O2	0.0397 (8)	0.0618 (11)	0.0395 (9)	-0.0154 (8)	0.0128 (7)	0.0018 (8)

Geometric parameters ( $\text{\AA}$ ,  $\text{^{\circ}}$ )

O1—C7	1.225 (2)	C11—H11B	0.9900
N1—C7	1.384 (2)	C12—C13	1.381 (3)
N1—C6	1.397 (2)	C12—C17	1.384 (3)
N1—C8	1.452 (2)	C13—C14	1.390 (3)
N2—C7	1.379 (2)	C13—H13	0.9500
N2—C1	1.395 (2)	C14—C15	1.373 (3)
N2—C18	1.450 (2)	C14—H14	0.9500
N3—N4	1.314 (2)	C15—C16	1.385 (4)
N3—C10	1.358 (3)	C15—H15	0.9500
N4—N5	1.347 (2)	C16—C17	1.377 (3)
N5—C9	1.356 (2)	C16—H16	0.9500
N5—C11	1.452 (2)	C17—H17	0.9500
C1—C2	1.381 (3)	C18—C19	1.510 (3)
C1—C6	1.397 (3)	C18—H18A	0.9900
C2—C3	1.392 (3)	C18—H18B	0.9900
C2—H2	0.9500	C19—C20	1.383 (3)
C3—C4	1.384 (3)	C19—C24	1.386 (3)
C3—H3	0.9500	C20—C21	1.387 (3)
C4—C5	1.397 (3)	C20—H20	0.9500
C4—H4	0.9500	C21—C22	1.373 (3)
C5—C6	1.379 (3)	C21—H21	0.9500
C5—H5	0.9500	C22—C23	1.382 (3)
C8—C9	1.494 (3)	C22—H22	0.9500
C8—H8A	0.9900	C23—C24	1.383 (3)
C8—H8B	0.9900	C23—H23	0.9500
C9—C10	1.368 (3)	C24—H24	0.9500
C10—H10	0.9500	O2—H2A	0.8700
C11—C12	1.507 (3)	O2—H2B	0.8701
C11—H11A	0.9900		
O2···O1 <sup>i</sup>	2.865 (2)	C10···H5	2.98
O2···C17 <sup>i</sup>	3.192 (3)	C11···H8B	2.90

O2···N3	2.892 (2)	C14···H20	2.83
O1···H8B	2.55	C18···H2	2.98
O1···H11B	2.81	C22···H16 <sup>vii</sup>	2.98
O1···H18A	2.56	C22···H13 <sup>vi</sup>	2.97
O1···H18A <sup>ii</sup>	2.87	C23···H16 <sup>vii</sup>	2.97
O2···H5 <sup>iii</sup>	2.64	H2···N4 <sup>viii</sup>	2.78
O2···H11B <sup>i</sup>	2.77	H2A···N4	2.62
O2···H17 <sup>i</sup>	2.71	H2A···N3	2.04
N4···C13	3.200 (3)	H2B···O1 <sup>i</sup>	2.00
N2···H20	2.60	H2B···H11B <sup>i</sup>	2.48
N4···H13	2.73	H3···H15 <sup>vi</sup>	2.48
N5···H13	2.52	H4···H18A <sup>ix</sup>	2.57
C1···C20	3.557 (3)	H5···H10	2.44
C2···C6 <sup>iv</sup>	3.542 (3)	H8A···N4 <sup>v</sup>	2.67
C3···C7 <sup>iv</sup>	3.540 (3)	H8B···H11B	2.27
C5···C9	3.592 (3)	H10···O2 <sup>v</sup>	2.48
C9···C5	3.592 (3)	H10···H17 <sup>ix</sup>	2.46
C10···O2 <sup>v</sup>	3.402 (3)	H11A···C15 <sup>v</sup>	2.92
C11···C15 <sup>v</sup>	3.421 (3)	H11A···H17	2.51
C14···C20	3.505 (3)	H16···H23 <sup>vii</sup>	2.44
C2···H18B	2.98	H16···H22 <sup>vii</sup>	2.46
C3···H15 <sup>vi</sup>	2.88	H18A···H18A <sup>ii</sup>	2.19
C8···H11B	2.79	H18B···H24	2.43
C8···H5	2.99	H24···N3 <sup>viii</sup>	2.76
C7—N1—C6	109.72 (15)	N5—C11—H11B	108.9
C7—N1—C8	123.68 (15)	C12—C11—H11B	108.9
C6—N1—C8	125.96 (15)	H11A—C11—H11B	107.7
C7—N2—C1	109.90 (15)	C13—C12—C17	119.63 (19)
C7—N2—C18	123.91 (16)	C13—C12—C11	123.39 (18)
C1—N2—C18	125.82 (16)	C17—C12—C11	116.99 (18)
N4—N3—C10	108.55 (17)	C12—C13—C14	120.1 (2)
N3—N4—N5	107.17 (16)	C12—C13—H13	119.9
N4—N5—C9	111.14 (15)	C14—C13—H13	119.9
N4—N5—C11	118.44 (16)	C15—C14—C13	119.9 (2)
C9—N5—C11	130.35 (17)	C15—C14—H14	120.1
C2—C1—N2	131.12 (19)	C13—C14—H14	120.1
C2—C1—C6	121.84 (18)	C14—C15—C16	120.0 (2)
N2—C1—C6	106.99 (16)	C14—C15—H15	120.0
C1—C2—C3	116.5 (2)	C16—C15—H15	120.0
C1—C2—H2	121.7	C17—C16—C15	120.2 (2)
C3—C2—H2	121.7	C17—C16—H16	119.9
C4—C3—C2	121.7 (2)	C15—C16—H16	119.9
C4—C3—H3	119.1	C16—C17—C12	120.1 (2)
C2—C3—H3	119.1	C16—C17—H17	119.9
C3—C4—C5	121.65 (19)	C12—C17—H17	119.9
C3—C4—H4	119.2	N2—C18—C19	114.52 (15)
C5—C4—H4	119.2	N2—C18—H18A	108.6

C6—C5—C4	116.6 (2)	C19—C18—H18A	108.6
C6—C5—H5	121.7	N2—C18—H18B	108.6
C4—C5—H5	121.7	C19—C18—H18B	108.6
C5—C6—C1	121.66 (18)	H18A—C18—H18B	107.6
C5—C6—N1	131.39 (18)	C20—C19—C24	118.34 (19)
C1—C6—N1	106.93 (15)	C20—C19—C18	122.54 (18)
O1—C7—N2	127.11 (18)	C24—C19—C18	119.06 (17)
O1—C7—N1	126.52 (18)	C19—C20—C21	120.8 (2)
N2—C7—N1	106.37 (15)	C19—C20—H20	119.6
N1—C8—C9	112.68 (15)	C21—C20—H20	119.6
N1—C8—H8A	109.1	C22—C21—C20	120.2 (2)
C9—C8—H8A	109.1	C22—C21—H21	119.9
N1—C8—H8B	109.1	C20—C21—H21	119.9
C9—C8—H8B	109.1	C21—C22—C23	119.6 (2)
H8A—C8—H8B	107.8	C21—C22—H22	120.2
N5—C9—C10	103.82 (17)	C23—C22—H22	120.2
N5—C9—C8	125.29 (17)	C22—C23—C24	120.0 (2)
C10—C9—C8	130.88 (18)	C22—C23—H23	120.0
N3—C10—C9	109.31 (18)	C24—C23—H23	120.0
N3—C10—H10	125.3	C23—C24—C19	121.0 (2)
C9—C10—H10	125.3	C23—C24—H24	119.5
N5—C11—C12	113.37 (16)	C19—C24—H24	119.5
N5—C11—H11A	108.9	H2A—O2—H2B	103.2
C12—C11—H11A	108.9		
C10—N3—N4—N5	-0.7 (2)	C11—N5—C9—C10	177.1 (2)
N3—N4—N5—C9	0.3 (2)	N4—N5—C9—C8	-178.77 (17)
N3—N4—N5—C11	-176.95 (17)	C11—N5—C9—C8	-1.9 (3)
C7—N2—C1—C2	175.59 (19)	N1—C8—C9—N5	86.6 (2)
C18—N2—C1—C2	2.4 (3)	N1—C8—C9—C10	-92.1 (3)
C7—N2—C1—C6	-1.9 (2)	N4—N3—C10—C9	0.9 (3)
C18—N2—C1—C6	-175.07 (17)	N5—C9—C10—N3	-0.7 (2)
N2—C1—C2—C3	-177.86 (19)	C8—C9—C10—N3	178.24 (19)
C6—C1—C2—C3	-0.7 (3)	N4—N5—C11—C12	73.3 (2)
C1—C2—C3—C4	-0.4 (3)	C9—N5—C11—C12	-103.4 (2)
C2—C3—C4—C5	1.1 (3)	N5—C11—C12—C13	7.5 (3)
C3—C4—C5—C6	-0.8 (3)	N5—C11—C12—C17	-172.44 (19)
C4—C5—C6—C1	-0.2 (3)	C17—C12—C13—C14	-1.9 (3)
C4—C5—C6—N1	178.04 (18)	C11—C12—C13—C14	178.1 (2)
C2—C1—C6—C5	1.0 (3)	C12—C13—C14—C15	-0.6 (3)
N2—C1—C6—C5	178.79 (17)	C13—C14—C15—C16	2.4 (4)
C2—C1—C6—N1	-177.65 (17)	C14—C15—C16—C17	-1.7 (4)
N2—C1—C6—N1	0.13 (19)	C15—C16—C17—C12	-0.8 (4)
C7—N1—C6—C5	-176.8 (2)	C13—C12—C17—C16	2.6 (3)
C8—N1—C6—C5	-5.8 (3)	C11—C12—C17—C16	-177.4 (2)
C7—N1—C6—C1	1.7 (2)	C7—N2—C18—C19	109.6 (2)
C8—N1—C6—C1	172.72 (16)	C1—N2—C18—C19	-78.2 (2)
C1—N2—C7—O1	-176.56 (19)	N2—C18—C19—C20	-24.7 (3)

C18—N2—C7—O1	−3.2 (3)	N2—C18—C19—C24	158.15 (18)
C1—N2—C7—N1	2.9 (2)	C24—C19—C20—C21	−0.8 (3)
C18—N2—C7—N1	176.23 (16)	C18—C19—C20—C21	−178.0 (2)
C6—N1—C7—O1	176.65 (18)	C19—C20—C21—C22	−0.2 (4)
C8—N1—C7—O1	5.4 (3)	C20—C21—C22—C23	0.7 (4)
C6—N1—C7—N2	−2.83 (19)	C21—C22—C23—C24	−0.1 (4)
C8—N1—C7—N2	−174.11 (16)	C22—C23—C24—C19	−1.0 (3)
C7—N1—C8—C9	−111.65 (19)	C20—C19—C24—C23	1.4 (3)
C6—N1—C8—C9	78.5 (2)	C18—C19—C24—C23	178.7 (2)
N4—N5—C9—C10	0.2 (2)		

Symmetry codes: (i)  $x-1, -y+1/2, z-1/2$ ; (ii)  $-x+2, -y+1, -z+2$ ; (iii)  $x, -y+1/2, z-1/2$ ; (iv)  $-x+1, -y+1, -z+2$ ; (v)  $x, -y+1/2, z+1/2$ ; (vi)  $-x+1, -y+1, -z+1$ ; (vii)  $-x+2, -y+1, -z+1$ ; (viii)  $-x+1, y+1/2, -z+3/2$ ; (ix)  $x-1, y, z$ .

#### Hydrogen-bond geometry ( $\text{\AA}$ , $^\circ$ )

$C_g$  is the centroid of the triazole ring  $C$  (C9/C10/N3–N5).

$D-\text{H}\cdots A$	$D-\text{H}$	$\text{H}\cdots A$	$D\cdots A$	$D-\text{H}\cdots A$
O2—H2A $\cdots$ N3	0.87	2.04	2.892 (2)	166
O2—H2B $\cdots$ O1 <sup>i</sup>	0.87	2.00	2.865 (2)	176
C10—H10 $\cdots$ O2 <sup>v</sup>	0.95	2.48	3.402 (3)	164
C13—H13 $\cdots$ $C_g$	0.95	2.83	3.451 (3)	124

Symmetry codes: (i)  $x-1, -y+1/2, z-1/2$ ; (v)  $x, -y+1/2, z+1/2$ .